

## Ecological speciation in sympatric palms: 3. Genetic map reveals genomic islands underlying species divergence in *Howea*

Papadopoulos, Alexander S. T.; Igea, Javier; Dunning, Luke T; Osborne, Owen; Quan, Xueping; Pellicer, Jaume; Turnbull, Colin; Hutton, Ian; Baker, William J.; Butlin, Roger K.; Savolainen, Vincent

### Evolution

DOI:  
[10.1111/evo.13796](https://doi.org/10.1111/evo.13796)

Published: 01/09/2019

Peer reviewed version

[Cyswllt i'r cyhoeddiad / Link to publication](#)

*Dyfyniad o'r fersiwn a gyhoeddwyd / Citation for published version (APA):*

Papadopoulos, A. S. T., Igea, J., Dunning, L. T., Osborne, O., Quan, X., Pellicer, J., Turnbull, C., Hutton, I., Baker, W. J., Butlin, R. K., & Savolainen, V. (2019). Ecological speciation in sympatric palms: 3. Genetic map reveals genomic islands underlying species divergence in *Howea*. *Evolution*, 73(9), 1986-1995. <https://doi.org/10.1111/evo.13796>

### Hawliau Cyffredinol / General rights

Copyright and moral rights for the publications made accessible in the public portal are retained by the authors and/or other copyright owners and it is a condition of accessing publications that users recognise and abide by the legal requirements associated with these rights.

- Users may download and print one copy of any publication from the public portal for the purpose of private study or research.
- You may not further distribute the material or use it for any profit-making activity or commercial gain
- You may freely distribute the URL identifying the publication in the public portal ?

### Take down policy

If you believe that this document breaches copyright please contact us providing details, and we will remove access to the work immediately and investigate your claim.

## 1 BRIEF COMMUNICATION

2

### 3 Ecological speciation in sympatric palms: 3. Genetic map reveals genomic islands underlying 4 species divergence in *Howea*

5

#### 6 Abstract

7 Although it is now widely accepted that speciation can occur in the face of continuous gene flow,  
8 with little or no spatial separation, the mechanisms and genomic architectures that permit such  
9 divergence are still debated. Here, we examined speciation in the face of gene flow in the *Howea*  
10 palms of Lord Howe Island, Australia. We built a genetic map using a novel method applicable to  
11 long-lived tree species, combining it with double digest restriction-site associated DNA sequencing  
12 of multiple individuals. Based upon various metrics, we detected 46 highly differentiated regions  
13 throughout the genome, four of which contained genes with functions that are particularly relevant  
14 to the speciation scenario for *Howea*, specifically salt and drought tolerance.

15

#### 16 Introduction

17 We investigated the genomic basis of speciation in *Howea* palms, which is a genus of only two  
18 species endemic to a minute oceanic island, Lord Howe Island (LHI), in the Tasman sea. LHI sits  
19 600 km off mainland Australia and is less than 16 km<sup>2</sup>, meaning that for any pair of endemic sister  
20 species that have diverged within the lifetime of the island (6.9 my), an allopatric phase in their  
21 divergence is unlikely (Savolainen *et al.* 2006; Papadopoulos *et al.* 2011). Hence, *Howea* is a solid  
22 example of speciation in sympatry (Savolainen *et al.* 2006; Coyne 2011; Papadopoulos *et al.* 2011,  
23 2019). Furthermore, it has been hypothesised that the two *Howea* species diverged in sympatry as a  
24 result of ecological speciation facilitated by soil adaptation and a shift in flowering phenology (Fig.  
25 1; Savolainen *et al.* 2006; Babik *et al.* 2009; Papadopoulos *et al.* 2011, 2013b, 2014; Hipperson *et al.*  
26 2016). *Howea* is widespread on LHI, although *H. belmoreana* is restricted to the older volcanic  
27 rocks whereas *H. forsteriana* is found predominantly on Pleistocene calcareous deposits  
28 (calcareous) around the coast (Savolainen *et al.* 2006; Woodroffe *et al.* 2006; Papadopoulos *et al.*  
29 2013). Marked flowering time differences between the species indicate that prezygotic isolation is  
30 now strong and current levels of gene flow are low (Savolainen *et al.* 2006; Babik *et al.* 2009;  
31 Dunning *et al.* 2016; Hipperson *et al.* 2016; Papadopoulos *et al.* 2019). Indirect evidence of post-  
32 zygotic isolation due to selection against juvenile hybrids supports the hypothesis that divergent  
33 selection has influenced the speciation process (Hipperson *et al.* 2016). Given that the distributions  
34 of *Howea* palms overlap extensively and that *Howea* is wind pollinated, speciation is likely to have  
35 occurred in the face of gene flow, which has reduced quickly as divergence progressed (Savolainen

*et al.* 2006; Babik *et al.* 2009; Papadopoulos *et al.* 2011, 2013, 2014, 2019). Here, we built a genetic map using a novel method applicable to long-lived tree species, combining it with double digest restriction-site associated DNA sequencing of multiple individuals, and we then examined the landscape of genomic differentiation that has arisen during and after speciation in *Howea* palms.

## Material and Methods

### DNA EXTRACTION

For linkage mapping, a single, wild *H. belmoreana* tree was selected on LHI, and leaf tissue was collected and preserved in silica gel. Ninety-four immature seeds were collected from this tree, dissected, and the endosperm tissue was removed and preserved in RNAlater (Sigma-Aldrich). Genomic DNA was then extracted using CTAB (Doyle & Doyle 1987) and purified using a caesium chloride gradient and dialysis. DNA samples were further cleaned and concentrated using DNeasy Mini spin columns (Qiagen). For the genome scan, leaf tissue was collected and preserved in silica gel from 42 *H. belmoreana* and 54 *H. forsteriana* individuals sampled at Far Flats, a plot on LHI where both species co-occur (Papadopoulos *et al.* 2019). For shotgun sequencing, a single, wild collected *H. forsteriana* individual was used. Genomic DNA was extracted from these 97 individuals using DNeasy Plant Mini kits (Qiagen).

### GENOTYPING AND LINKAGE MAP

Double digest RAD-sequencing (ddRAD) was performed following Papadopoulos *et al.* (2019). For the map, we genotyped a mother tree and 94 of its seeds. During the formation of the female megagametophyte a single cell undergoes meiosis and programmed cell death eliminates three of the four descendent haploid spores (Fig. S1). Three sequential mitotic nuclear divisions take place in the remaining megaspore to produce eight nuclei. Cellular division produces seven cells that make up the embryo sac, one of which – the central cell - contains two polar nuclei (Sundaresan & Alandete-Saez 2010). When fertilised, this homo-diploid cell develops into the triploid endosperm containing a single copy of the paternal genome and two identical copies of the maternal genome. Identification of which maternal allele is inherited by the offspring at any given heterozygous position in the mother was achieved by ddRAD sequencing of the maternal and endosperm tissue. The 2:1 ratio of maternal to paternal alleles is maintained in the relative read depth of alleles at each locus in the endosperm, allowing the maternally inherited allele at each locus to be determined in each seed sample (Fig. S1). The raw sequencing data were processed and individuals genotyped using components of the *STACKS* (Catchen *et al.* 2011) pipeline, *perl* and *R* scripts (R Development

Core Team 2019). The ‘process-radtags’ component of *STACKS* was used to de-multiplex the barcoded samples in each library, remove tags of low quality, with ambiguous barcodes or missing base calls, and truncate each sequence to 95 bp. The paired ends of each read were then merged into a single contiguous sequence to minimise the inclusion of paralogous sequences in the same RAD loci in subsequent steps. The genotyping process was composed of four main steps: (i) construction of a reliable, high coverage catalogue of heterozygous sites in the maternal tree; (ii) genotyping of endosperm tissue at these sites; (iii) addition of loci/haplotypes present in trees from the LHI site to the maternal catalogue; and (iv) genotyping of the wild trees. First (i), to remove highly similar clusters of *STACKS* and error prone loci from the maternal dataset the *STACKS* pipeline was run using at least five exactly matching reads to create a stack, allowing one mismatch between stacks to create a locus, allowing up to 200 stacks to form a single locus, disabling the deleveraging algorithm and disabling haplotype calling from secondary reads. Reads assigned to loci composed of more than two haplotypes were then removed from the dataset. The remaining reads were then processed using the *denovo\_map.pl* perl wrapper for *STACKS* to generate a catalogue of loci and haplotypes present in the mother using at least 50 exactly matching reads to create a stack and allowing three mismatches between stacks to create a locus. (ii) Reads for each endosperm tissue were assembled into loci using *USTACKS* (minimum depth to create a stack = 10, mismatches = 3) and these were then mapped to the maternal catalogue using *SSTACKS*. For all heterozygous loci in the mother, the two haplotypes in the endosperms were randomly assigned as an A or B allele and the read depths of haplotypes were extracted for each seed using custom *perl* scripts. To determine the maternally inherited allele (A or B) in each seed, the relative read depth of the A allele at each locus (read depth of A/read depth of A + B) was analysed using the *kmeans* clustering algorithm in R with 4 predefined clusters (corresponding to triploid genotypes of AAA = 1.00, AAB = 0.66, BBA = 0.33 and BBB = 0.00). (iii) To expand the catalogue to encompass haplotypes present in both *Howea* species, the Far Flats samples were assembled into loci using *USTACKS* (-m20, -M3) and these stacks were merged into the existing catalogue allowing 3 mismatches between loci in different individuals. (iv) To genotype the Far Flats individuals, loci were assembled with lower coverage in *USTACKS* (-m5, -M3) and these stacks were mapped to the catalogue loci. For the genome scan analyses, haplotypes of these individuals were extracted for loci included in the linkage map. Genotypic data for the *H. belmoreana* seeds were initially processed using the *R/qtl* (Broman *et al.* 2003) package. Four individuals were excluded due to high levels of missing data. After exclusion of these samples, loci with more than 22 missing genotypes out of 90 progeny were also removed from further analysis. The remaining 3,772 loci were phased and assembled into linkage groups using the *formlinkagegroups* function with a minimum logarithm of odds threshold of 7.0 and maximum recombination fraction of 0.25. The loci within each assembled linkage group

106 were then ordered in *JoinMap* v4.1 (Kyazma) using the regression mapping algorithm (three  
107 rounds), and inter-marker distances were calculated in centimorgans (cM) using the Kosambi  
108 mapping function. The mean coverage of mapped loci was 1,117 reads in the mother (s.d. +/- 1,145)  
109 and 176 (s.d. +/- 89) in the endosperm. Unequivocal homozygote genotypes accounted for 51% of  
110 endosperm allele calls, 32% of calls were derived from proportional differences between alleles and  
111 17% were treated as missing data.

112

## 113 IDENTIFYING GENOMIC ISLANDS

114 Differentiation (i.e.,  $F_{ST}$ ; Weir & Cockerham 1984) between *H. belmoreana* and *H. forsteriana* was  
115 calculated at each ddRAD locus using the *diveRsity* package in *R* (Keenan *et al.* 2013). Divergence  
116 ( $d_{XY}$ ) was also calculated for each locus using equation 10.20 of Nei (1987). Genome-wide  
117 distributions of  $F_{ST}$  and  $d_{XY}$  were generated using a local Gaussian kernel smoothing technique  
118 within each chromosome (Hohenlohe *et al.* (2010). Kernel smoothing was performed using the  
119 *ksmooth* function in *R* with a bandwidth value of 2 cM, defined as the standard deviation of the  
120 kernel. The bandwidth of 2 cM was chosen because it is similar to the average distance between the  
121 markers (1.6 cM). To identify genomic islands with both high  $F_{ST}$  and  $d_{XY}$ , *fastsimcoal2* was used  
122 to generate a null distribution of expected  $F_{ST}$  and  $d_{XY}$  values (i.e. without selection) that  
123 incorporated a demographic scenario (Papadopoulos *et al.* 2019) and the position of markers in the  
124 genetic map. Under the best fitting *fastsimcoal2* model (a model with initial strong gene flow  
125 followed by a reduced gene flow, model 5 in Papadopoulos *et al.* 2019; see Table S1 for parameters),  
126 we simulated the same number of 190 bp DNA fragments as contained in the genetic map with the  
127 positions preserved by separating simulated loci by the same recombination distances as in the map  
128 (i.e., recombination rate between loci varied across the genome). Within fragments, recombination  
129 was fixed at the genome wide average ( $6.85 \times 10^{-9}$  base<sup>-1</sup> generation<sup>-1</sup>). Each chromosome was  
130 simulated 1,000 times separately. Kernel smoothed  $F_{ST}$  values were calculated for each simulation  
131 using the methods applied to the observed data above. These data were used to calculate P-values at  
132 each centimorgan, and outlier  $F_{ST}$  islands were identified at alpha = 0.05. Outlier  $d_{XY}$  regions were  
133 identified as those positions with  $d_{XY}$  values in the 90<sup>th</sup> percentile of the observed data. Observed  
134 rather than simulated data was used as the random assignment of mutation in the simulation lead to  
135 very broad confidence intervals for  $d_{XY}$ . To define the full extent of the high  $F_{ST} + d_{XY}$  islands –  
136 these islands were joined or extended only if the position next to an  $F_{ST} + d_{XY}$  outlier had a high  
137 (but not significant) probability of being an  $F_{ST}$  outlier (assessed using Hidden Markov Models,  
138 HMM) and also coincided with a region of high  $d_{XY}$ . To do this,  $F_{ST}$  P-values were converted into  
139 z-scores using *qnorm* and three hidden states were fitted to detect regions of the genome with low,  
140 intermediate and high probabilities of belonging to an outlier region. For each state, a Gaussian

141 distribution of the z-scores was assumed. Means and standard deviations for each hidden state, as  
142 well as the transition matrix defining probabilities of transferring from one state to another, were all  
143 estimated from the data. Direct transitions from low to high states were not permitted. Parameters  
144 were estimated using the Baum-Welch algorithm and the probable sequence of hidden states was  
145 determined from the data and parameter estimates using the Verbiti algorithm. The results of the  
146 HMM procedure were only used to define the size of the regions identified at  $P < 0.05$ , rather than  
147 locate the position of islands. An island was only extended when an adjacent position (i) was  
148 assigned the high  $F_{ST}$  state by the HMM and (ii) was an outlier  $d_{XY}$  position.

149

## 150 ESTIMATION OF RECOMBINATION RATE

151 To estimate recombination rates in genomic islands versus the rest of the genome, we assembled a  
152 draft genome of *Howea*. We estimated the genome size of *H. forsteriana* and *H. belmoreana*  
153 following the one-step flow cytometry procedure described by Doležel *et al.* (2007). Then, a  
154 shotgun genome assembly was performed for *H. forsteriana*. A total of 432.98 Gigabases (Gb) of  
155 cleaned, paired-end, Illumina reads (49-150 bp reads, insert sizes = 170 bp, 250 bp, 800 bp, 2  
156 kilobases (kb), 5 kb, 10 kb and 20 kb) were assembled into genomic contigs using *SOAPdenovo*  
157 (Luo *et al.* 2012). *SSPACE* (Boetzer *et al.* 2011) was then used to extend and scaffold contigs.  
158 Summary statistics for the shotgun assembly are provided in the supplementary material (Table S2).  
159 *BUSCO* (Simão *et al.* 2015) analysis was performed in genome mode using the Embryophyta  
160 BUSCOs (Benchmarking Universal Single-Copy Orthologs) to assess genome completeness.  
161 Consensus sequences of the ddRAD markers included in the genetic map were mapped to genomic  
162 scaffolds using *BLASTn* (Camacho *et al.* 2009), retaining only the best hits. As suggested by Tang  
163 *et al.* (2015), scaffolds ( $n = 3,980$  and total length = 0.42 Gb) were ordered based on the average  
164 map location of the ddRAD markers for each scaffold. The physical length of each chromosome  
165 was calculated using the proportion of the total length of scaffolds (0.42 Gb) that mapped to that  
166 chromosome. As only 13.3% of the genome is covered by our scaffolds, we then estimated the  
167 length of that chromosome as the corresponding proportion of the total genome size of *H.*  
168 *forsteriana* (estimated here as 3.15 Gb). Finally, we calculated the recombination rate as the genetic  
169 distance from the map divided by the estimated physical length of a given genomic region as above  
170 (chromosomes and genomic islands) in 10 cM sliding windows.

171

## 172 GENE CONTENT IN GENOMIC ISLANDS

173 To assign transcripts from the *Howea* reference transcriptome (Dunning *et al.* 2016) to genomic  
174 scaffolds, *BLASTn* was used with *max\_target\_seqs*=1 and an E-value cut-off of  $1 \times 10^{-20}$ . Only the  
175 highest scoring match for each transcript was retained. Using transcriptome data from Dunning *et*

176 *al.* (2016), the proportions of transcripts showing evidence of differential expression or signatures  
 177 of selection within and outside speciation islands were compared using Fisher's Exact Tests. This  
 178 was done using highly differentiated genes ( $F_{ST} > 0.8$ ), genes with evidence for positive selection  
 179 ( $d_N/d_S > 1$ ), and differentially expressed genes in any tissue (Dunning *et al.* 2016). The transcripts  
 180 from Dunning *et al.* (2016) were mapped to genomic scaffolds using *BLAT* with default settings  
 181 (Kent 2002). Alignments were then filtered to include only the best hit for each transcript and  
 182 alignments covering 80% of the transcript. Filtered *BLAT* alignments were then converted to  
 183 *AUGUSTUS* hints (Stanke *et al.* 2006). *AUGUSTUS* was used to predict genes in the genomic  
 184 scaffolds, using the transcript-derived hints and annotation training files from *Zea mays* using the  
 185 following settings: no UTR prediction, no in-frame stop codons, and gene prediction on both  
 186 strands. The resulting predicted amino acid sequences were *BLASTp*-searched against the  
 187 *Arabidopsis thaliana* proteome (Araport11\_genes.201606.pep downloaded on 31/01/17) and only  
 188 the best scoring hit from each predicted amino acid sequence was retained. Gene ontology (GO)  
 189 enrichment for genomic islands was compared to all scaffolded transcripts; this was performed for  
 190 both transcriptome-based (Dunning *et al.* 2016) and the above *AUGUSTUS*-based genome  
 191 annotations. To test for enrichment of GO terms among genes within particular genomic islands we  
 192 used the R package *TopGO* (Alexa *et al.* 2006) using the "elim" algorithm and Fisher's Exact tests  
 193 to assess significance. Preliminary assessment of gene functions in genomic islands was made from  
 194 The Arabidopsis Information Resource (TAIR) descriptions of gene functions, GO terms and  
 195 associated references. Further published records of functional assessments were acquired from the  
 196 TAIR known phenotypes database (<https://www.arabidopsis.org>), the drought stress genes database  
 197 ([http://pgsb.helmholtz-muenchen.de/droughtdb/drought\\_db.html](http://pgsb.helmholtz-muenchen.de/droughtdb/drought_db.html)) and the flowering interactive  
 198 database (<http://www.phytosystems.ulg.ac.be/florid/>). Finally, systematic web searches were  
 199 performed using gene names with and without the terms "stress" and "flowering", given the  
 200 speciation scenario for *Howea* (Fig. 1).

201

## 202 **Results and discussion**

203

### 204 **GENE FLOW AND GENOMIC DIFFERENTIATION**

205 The linkage map contains 3,772 ddRAD loci ordered onto 16 linkage groups corresponding to the  
 206 16 pairs of chromosomes in *Howea* (Savolainen *et al.* 2006) and spanning 2,399 cM (0.70 cM/Mb  
 207 or 1.42 Mb/cM; Fig. 2 and S2, Table S3). Across the map, we observed a positive correlation  
 208 between  $F_{ST}$  and  $d_{XY}$  ( $p < 0.0001$ ,  $r^2 = 0.18$ ; Figs. S3 and S4), which, in these relatively recently  
 209 diverged species, may be an indication that gene flow has played a role in shaping genomic  
 210 differentiation. To characterise the genomic landscape,  $F_{ST}$  and  $d_{XY}$  were calculated for 1,498 high-

quality ddRAD loci in the map, which were present in both species (genome wide,  $F_{ST} = 0.46$ ,  $d_{XY} = 7.6 \times 10^{-3}$ ). Genetic differentiation during sympatric speciation should be substantially greater for loci that have been subject to divergent selection than for loci in neutral regions (Wu 2001). In the course of speciation with gene flow, genomic regions in proximity with those barrier loci that are the target of selection may experience reduced effective gene flow. Meanwhile, the rest of the genome would still be subject to the homogenising effects of genetic exchange (Nosil *et al.* 2008; Via & West 2008; Soria-Carrasco *et al.* 2014). This may lead to a pattern of elevated differentiation ( $F_{ST}$ ) and divergence ( $d_{XY}$ ) in regions containing barrier loci compared to the rest of the genome (Hohenlohe *et al.* 2010; Ellegren *et al.* 2012; Nadeau *et al.* 2012; Martin *et al.* 2013; Renaut *et al.* 2013; Poelstra *et al.* 2014). These patterns of heterogeneous genomic differentiation have been used in attempts to identify regions of the genome that harbour barrier loci responsible for adaptation and speciation (Ellegren *et al.* 2012; Nadeau *et al.* 2012; Martin *et al.* 2013; Poelstra *et al.* 2014). However, there are several complicating factors that may mean that these regions do not act as barriers to gene flow (see sections below for discussion of these; Noor & Bennett 2010; Turner & Hahn 2010; Cruickshank & Hahn 2014; Ravinet *et al.* 2017). Here, high- $F_{ST}$  islands (mean  $F_{ST} = 0.87$ , range = 0.64 – 0.99, mean  $d_{XY} = 9.9 \times 10^{-3}$ , range =  $5.0 \times 10^{-3} - 1.7 \times 10^{-2}$ ) were numerous (38 islands), relatively small (mean size = 1.7 cM, range = 1 – 5 cM) and accounted for 3.3% of the genome (total length = 80 cM; Table S4). In contrast, we detected only eight islands with both higher  $F_{ST}$  and  $d_{XY}$  (high- $F_{ST}+d_{XY}$ ) than the rest of the genome (mean  $F_{ST} = 0.88$ , range = 0.58 – 0.98, mean  $d_{XY} = 1.5 \times 10^{-2}$ , range =  $1.2 \times 10^{-2} - 2.0 \times 10^{-2}$ ; Welch's t-test,  $P < 0.0001$ ), which were located on seven pairs of chromosomes. These high- $F_{ST}+d_{XY}$  genomic islands were, on average, marginally larger (mean size = 2.38 cM, range = 1 – 4 cM; Mann-Whitney U test,  $P = 0.05$ ) than other high- $F_{ST}$  islands, and represented only 0.8% of the genome (19 cM, Table S5). A permutation test showed that high- $F_{ST}+d_{XY}$  islands were not the result of high- $F_{ST}$  and high- $d_{XY}$  positions co-occurring by chance ( $P < 0.0001$ ). These high- $F_{ST}+d_{XY}$  islands are more likely to have been involved in speciation in the face of gene flow than islands with high- $F_{ST}$  but no elevation in  $d_{XY}$  (Hohenlohe *et al.* 2010; Ellegren *et al.* 2012; Nadeau *et al.* 2012; Martin *et al.* 2013; Renaut *et al.* 2013; Poelstra *et al.* 2014). In both species, nucleotide diversity ( $\pi$ ) was significantly lower in high- $F_{ST}$  islands than the genome average (Table S6) as has been observed in other plants (Chapman *et al.* 2016), but was only lower in high- $F_{ST}+d_{XY}$  islands for *H. forsteriana*. In seven out of eight of high- $F_{ST}+d_{XY}$  islands,  $\pi$  was substantially lower in *H. forsteriana* than in *H. belmoreana*, a possible indication of a selective sweep having taken place in this species. The generally small size of high- $F_{ST}+d_{XY}$  islands indicates that these islands did not expand gradually over time, as would be expected under divergence hitchhiking theory when gene flow is ongoing (Via 2009; Feder *et al.* 2012; Rafajlović *et al.* 2016). Our results contrast with those in a comparable analysis of another



246 case of sympatric speciation, i.e., the cichlids of lake Massoko in Tanzania (Malinsky *et al.* 2015).  
247 In a whole genome analysis of these fish, and measuring  $F_{ST}$  and  $d_{XY}$  as here, 55 high- $F_{ST}+d_{XY}$   
248 islands were identified. This is substantially more than in the palms here and from a much smaller  
249 genome. Similar numbers of islands were found in flycatchers and many more in other systems  
250 (Ellegren *et al.* 2012; Renaut *et al.* 2013; Soria-Carrasco *et al.* 2014). This is likely to be, in part,  
251 due to the resolution of our map as we have probably missed finer scale islands ( $< 1\text{cM}$ ). However,  
252 it is noteworthy that in the Massoko cichlids, 27 islands formed clusters extending 5 - 45 cM across  
253 five linkage groups, which are larger than the islands detected in *Howea*, suggesting the resolution  
254 we use may be sufficient to detect a substantial proportion of the larger islands in our system.

255 An alternative explanation for high- $F_{ST}+d_{XY}$  islands has been proposed recently (Guerrero & Hahn  
256 2017). Guerrero and Hahn showed that these regions can be the result of balanced polymorphisms  
257 in the ancestral population that have been ‘sieved’ by the speciation process when different alleles  
258 are fixed in each descendent population. Because ancestral balanced polymorphisms have had  
259 longer to accumulate divergence than those that only diverged following speciation, this process is  
260 expected to have the most pronounced effect early in speciation ( $t < 2N_e$ ; where  $t$  = divergence time  
261 and  $N_e$  = effective population size). If sieved polymorphisms are responsible for these islands,  
262 then  $d_{XY}$  in these regions should substantially exceed the expected level of  $d_{XY}$  based on the time  
263 since speciation, which can be calculated as  $E(d_{XY}) = 2\mu t + \theta_{ANC}$  (where  $\mu$  = the neutral mutation  
264 rate and  $\theta_{ANC}$  = the ancestral level of diversity). Using respective estimates of  $t$  and  $\mu$  of 266,136  
265 and  $1.3 \times 10^{-8}$  from (Papadopoulos *et al.* 2019) and assuming  $\theta_{ANC} = 0$  (because of the bottleneck  
266 caused by long-distance colonisation of LHI), we arrive at an expected  $d_{XY}$  of  $6.9 \times 10^{-3}$ . This  
267 differs from the level of  $d_{XY}$  estimated from our map by only 0.0007, which may constitute the  
268 contribution of ancestral polymorphism to our estimate. Alternatively, this small discrepancy may  
269 arise if our estimate of  $t$  is wrong by approximately 100,000 years (within the 95% CI of  $t$ ) or if our  
270  $d_{XY}$  estimate is derived only from the subset of the data used for the demographic inference that was  
271 also included in the map. These estimates are substantially lower than our mean observed  $d_{XY}$  for  
272 high- $F_{ST}+d_{XY}$  islands ( $1.5 \times 10^{-2}$ ), but similar to that of the high- $F_{ST}$  only islands. These data may  
273 point to a role for sieved balanced polymorphisms in the origin of our high- $F_{ST}+d_{XY}$  islands, and  
274 that sympatric speciation may have been reliant on existing genetic variation in the ancestral  
275 population. However, we cannot rule out the possibility that some of these high- $F_{ST}+d_{XY}$  regions  
276 may contain sieved polymorphisms that did not play a direct role in the speciation process.

## 277 278 HIGH- $F_{ST}$ ISLANDS ARE IN REGIONS OF LOW RECOMBINATION

279 Whole genome shotgun sequencing for *H. forsteriana* produced 432.98 Gb of Illumina reads (126x  
280 coverage), which assembled into a total length of 3.15 Gb (contig N50 = 3783, scaffold N50 =

37,986; Table S2), similar to the genome size estimated from flow cytometry: For *H. forsteriana*,  
1C =  $3.50 \pm 0.01$  pg ( $3,423 \pm 9.78$  Mb); for *H. belmoreana*, 1C =  $3.08 \pm 0.02$  pg ( $3,012.24 \pm 19.56$   
Mb). BUSCO (Simão *et al.* 2015) analysis of the assembled genome found that 73.2% of BUSCOs  
were complete.

In four of eight high- $F_{ST}+d_{XY}$  islands, the genetic distance (cM) per Mb was lower, i.e.  
recombination rate was lower, than the average rate for the rest of the chromosome where the island  
was located, but no different from a random draw (Table S3 and S5, sign test,  $P = 0.5$ ). As a whole,  
high- $F_{ST}+d_{XY}$  islands did not have significantly lower estimated recombination rates than the rest of  
the genome (Fig. 3, Welch's t-test,  $P = 0.39$ ), but high- $F_{ST}$  differentiation islands did ( $P < 0.0001$ ).  
In line with the findings in *Howea*, a recent analysis of sympatric populations of divergent  
stickleback ecotypes showed that signatures of adaptation were considerably more frequent in  
regions of low recombination when compared to the same ecotype in sympatry or parallel and  
divergent ecotypes in allopatry (Samuk *et al.* 2017). It has been proposed that limited marker  
resolution can result in a reduced ability to detect islands outside regions of low recombination  
(Lowry *et al.* 2017). Given the resolution of our data this is a possibility. However, not all of the  
high- $F_{ST}$  only islands detected fall within regions of low recombination and our null model  
explicitly accounts for the recombination distance between markers, suggesting this is unlikely to be  
the case. Furthermore, Samuk *et al.* (2017) compared whole genome and 'genotyping by  
sequencing' and found that the pattern of ecotype-associated divergence correlated with  
recombination rate was consistent between datasets, and therefore was not an artefact of low marker  
density. In addition, our high- $F_{ST}+d_{XY}$  islands are not associated with low recombination, indicating  
that their detection was not an artefact of limited marker density.

The association of high- $F_{ST}$  only islands with low recombination could be the result of  
linked selection (either background selection or hitchhiking) (Burri *et al.* 2015). If genomic  
diversity was largely shaped by linked selection, we would expect a positive correlation between  $\pi$   
and recombination rate; in fact, the opposite is observed across the whole genome (Fig. 4) as well as  
within both high- $F_{ST}$  and high- $F_{ST}+d_{XY}$  islands (Fig S5). Also,  $d_{XY}$  was negatively correlated with  
recombination rate (Fig. 4,  $P < 0.0001$ ) - a pattern that was also observed in sympatric stickleback  
ecotypes and interpreted as a joint effect of gene flow and divergent selection (Samuk *et al.* 2017).  
These findings are consistent with a limited role for linked selection in the evolution of  
heterogeneous differentiation in *Howea*. Instead, high- $F_{ST}$  only islands are more likely to have  
arisen as a product of selection after speciation.

313

STRESS AND FLOWERING TIME GENES ARE PRESENT IN SPECIATION ISLANDS

315 We detected 37 genes in high- $F_{ST}+d_{XY}$  islands, 19 of which could be annotated by comparison to  
316 the *Arabidopsis* Araport11 protein sequences. An additional 233 genes were located in high- $F_{ST}$   
317 only islands, of which we annotated 120. In total 5,309 genes were assigned to the genetic map, of  
318 which 3,020 were annotated, including 2,844 with GO terms. We then examined whether these  
319 islands were enriched for any GO terms. There was an excess of genes involved in responses to  
320 abiotic stimuli and catabolism of organic compounds in our annotated 120 (Table S7). We also  
321 evaluated whether genes that were found to be potentially involved in *Howea* speciation by  
322 Dunning *et al.* (2016) were present in our islands. Out of 2,250 such candidate genes that were  
323 included on our genetic map, 19 were found in high- $F_{ST}+d_{XY}$  islands (Table S8), although this did  
324 not represent a higher proportion than expected by chance (Fisher's exact test,  $P = 0.863$ ). Note that  
325 4,598 candidate genes from Dunning *et al.* (2016) were not found on the map, and these could still  
326 have been important during speciation. Furthermore, it may be that the transcriptome-derived  
327 candidate genes (Dunning *et al.* 2016) are regulated by genes within our high- $F_{ST}+d_{XY}$  islands.  
328 Alternatively, it is possible that some candidates were not involved in speciation, but diverged  
329 subsequently.

330 Finally, we performed a systematic review of the known functions of the 19 annotated genes  
331 in high- $F_{ST}+d_{XY}$  islands. We could ascribe 13 of these genes with functions relevant to the  
332 speciation scenario, that is, environmental stresses (including those stemming from soil preferences)  
333 and flowering time (Fig. 1 and Table S9). Three genes were linked to salt stress, four to drought  
334 stress, two to alterations in flowering time, three to osmotic stress, two to cold and three to light  
335 stresses (references in Table S9). High- $F_{ST}+d_{XY}$  islands No. 3.1, 5.1, 12.1 and 15.1 contained  
336 multiple genes with relevant functions (Table S9), and it is noteworthy that both islands 3.1 and  
337 15.1 contained genes with  $F_{ST} > 0.9$  (Dunning *et al.* 2016) as well as a combination of genes  
338 involved in both environmental responses and flowering time control. These are good candidate  
339 genes for adaptation and speciation as the habitat that *H. forsteriana* occupies is characterised by  
340 low soil moisture and increased salt, light and wind exposure (Papadopoulos *et al.* 2019).

341

## 342 REFERENCES

343

- 344 Alexa, A., Rahnenführer, J. & Lengauer, T. (2006). Improved scoring of functional groups from  
345 gene expression data by decorrelating GO graph structure. *Bioinformatics* 22: 1600–1607.
- 346 Babik, W., Butlin, R.K., Baker, W.J., Papadopoulos, A.S.T., Boulesteix, M., Anstett, M.C., *et al.*  
347 (2009). How sympatric is speciation in the *Howea* palms of Lord Howe Island? *Mol. Ecol.* 18:  
348 3629–3638.
- 349 Boetzer, M., Henkel, C. V., Jansen, H.J., Butler, D. & Pirovano, W. (2011). Scaffolding pre-

350 assembled contigs using SSPACE. *Bioinformatics* 27: 578–579.

351 Broman, K.W., Wu, H., Sen, Å. & Churchill, G.A. (2003). R/qtl: QTL mapping in experimental  
352 crosses. *Bioinformatics* 19: 889–890.

353 Burri, R., Nater, A., Kawakami, T., Mugal, C.F., Olason, P.I., Smeds, L., *et al.* (2015). Linked  
354 selection and recombination rate variation drive the evolution of the genomic landscape of  
355 differentiation across the speciation continuum of Ficedula flycatchers. *Genome Res.* 25:  
356 1656–1665.

357 Camacho, C., Coulouris, G., Avagyan, V., Ma, N., Papadopoulos, J., Bealer, K., *et al.* (2009).  
358 BLAST plus: architecture and applications. *BMC Bioinformatics* 10: 1.

359 Catchen, J.M., Amores, A., Hohenlohe, P., Cresko, W. & Postlethwait, J.H. (2011). Stacks:  
360 Building and Genotyping Loci De Novo From Short-Read Sequences. *G3 Genes, Genomes,*  
361 *Genet.* 1: 171–182.

362 Chapman, M.A., Hiscock, S.J. & Filatov, D.A. (2016). The genomic bases of morphological  
363 divergence and reproductive isolation driven by ecological speciation in Senecio (Asteraceae).  
364 *J. Evol. Biol.* 29: 98–113.

365 Coyne, J.A. (2011). Speciation in a small space. *Proc. Natl. Acad. Sci.* 108: 12975–12976.

366 Cruickshank, T.E. & Hahn, M.W. (2014). Reanalysis suggests that genomic islands of speciation  
367 are due to reduced diversity, not reduced gene flow. *Mol. Ecol.* 23: 3133–3157.

368 Doležel, J., Greilhuber, J. & Suda, J. (2007). Estimation of nuclear DNA content in plants using  
369 flow cytometry. *Nat. Protoc.* 2: 2233–44.

370 Doyle, J.J. & Doyle, J.L. (1987). A rapid DNA isolation procedure for small amounts of fresh leaf  
371 tissue. *Phytochem. Bull.* 19: 11–15.

372 Dunning, L.T., H. Hipperson, Baker, W.J., Butlin, R.K., Devaux, C., Hutton, I., *et al.* (2016).  
373 Ecological speciation in sympatric palms: 1. Gene expression, selection and pleiotropy. *J.*  
374 *Evol. Biol.* 29: 1472–1487.

375 Ellegren, H., Smeds, L., Burri, R., Olason, P.I., Backstrom, N., Kawakami, T., *et al.* (2012). The  
376 genomic landscape of species divergence in Ficedula flycatchers. *Nature* 491: 756–760. Nature  
377 Publishing Group, a division of Macmillan Publishers Limited. All Rights Reserved.

378 Feder, J.L., Egan, S.P. & Nosil, P. (2012). The genomics of speciation-with-gene-flow. *Trends*  
379 *Genet.* 28: 342–350. Elsevier Trends Journals.

380 Guerrero, R.F. & Hahn, M.W. (2017). Speciation as a sieve for ancestral polymorphism. *Mol. Ecol.*  
381 1–7.

382 Hipperson, H., Dunning, L.T., Baker, W.J., Butlin, R.K., Hutton, I., Papadopoulos, A.S.T.T., *et al.*  
383 (2016). Ecological speciation in sympatric palms: 2. Pre- and post-zygotic isolation. *J. Evol.*  
384 *Biol.* 29: 2143–2156.

385 Hohenlohe, P.A., Bassham, S., Etter, P.D., Stiffler, N., Johnson, E.A. & Cresko, W.A. (2010).  
 386 Population genomics of parallel adaptation in threespine stickleback using sequenced RAD  
 387 tags. *PLoS Genet* 6: e1000862. Public Library of Science.  
 388 Keenan, K., McGinnity, P., Cross, T.F., Crozier, W.W. & Prodöhl, P.A. (2013). diveRsity: An R  
 389 package for the estimation and exploration of population genetics parameters and their  
 390 associated errors. *Methods Ecol. Evol.* 4: 782–788.  
 391 Kent, W.J. (2002). BLAT — The BLAST -Like Alignment Tool. *Genome Res.* 12: 656–664.  
 392 Lowry, D.B., Hoban, S., Kelley, J.L., Lotterhos, K.E., Reed, L.K., Antolin, M.F., *et al.* (2017).  
 393 Breaking RAD: an evaluation of the utility of restriction site-associated DNA sequencing for  
 394 genome scans of adaptation. *Mol. Ecol. Resour.* 17: 142–152.  
 395 Luo, R., Liu, B., Xie, Y., Li, Z., Huang, W., Yuan, J., *et al.* (2012). SOAPdenovo2: an empirically  
 396 improved memory-efficient short-read de novo assembler. *Gigascience* 1: 18.  
 397 Malinsky, M., Challis, R.J., Tyers, A.M., Schiffels, S., Terai, Y., Ngatunga, B.P., *et al.* (2015).  
 398 Genomic islands of speciation separate cichlid ecomorphs in an East African crater lake.  
 399 *Science* (80-. ). 350: 1493–1498.  
 400 Martin, S.H., Dasmahapatra, K.K., Nadeau, N.J., Salazar, C., Walters, J.R., Simpson, F., *et al.*  
 401 (2013). Genome-wide evidence for speciation with gene flow in *Heliconius* butterflies.  
 402 *Genome Res.* 23: 1817–1828.  
 403 Nadeau, N.J., Whibley, A., Jones, R.T., Davey, J.W., Dasmahapatra, K.K., Baxter, S.W., *et al.*  
 404 (2012). Genomic islands of divergence in hybridizing *Heliconius* butterflies identified by  
 405 large-scale targeted sequencing. *Philos. Trans. R. Soc. B Biol. Sci.* 367: 343–353.  
 406 Nei, M. (1987). *Molecular evolutionary genetics*. Columbia university press.  
 407 Noor, M.A.F. & Bennett, S.M. (2010). Islands of speciation or mirages in the desert? Examining the  
 408 role of restricted recombination in maintaining species. *Heredity (Edinb)*. 103: 439–444.  
 409 Nosil, P., Egan, S.P. & Funk, D.J. (2008). Heterogeneous genomic differentiation between walking-  
 410 stick ecotypes: ‘isolation-by-adaptation’ and multiple roles for divergent selection. *Evolution*  
 411 (*N. Y.*) 62: 316–336.  
 412 Papadopoulos, A.S.T., Baker, W.J., Crayn, D., Butlin, R.K., Kynast, R.G., Hutton, I., *et al.* (2011).  
 413 Speciation with gene flow on Lord Howe Island. *Proc. Natl. Acad. Sci. U. S. A.* 108: 13188–  
 414 13193.  
 415 Papadopoulos, A.S.T., Igea, J., Smith, T.P., Osborne, O., Dunning, L., Turnbull, C., *et al.* (2019).  
 416 Ecological speciation in sympatric palms: 4. Demographic analyses support that *Howea* did  
 417 speciate in the face of high gene flow. *Evolution (in revision)*.  
 418 Papadopoulos, A.S.T., Kaye, M., Devaux, C., Hipperson, H., Lighten, J., Dunning, L.T., *et al.*  
 419 (2014). Evaluation of genetic isolation within an island flora reveals unusually widespread

420 local adaptation and supports sympatric speciation. *Philos. Trans. R. Soc. B Biol. Sci.* 369:  
421 20130342.

422 Papadopoulos, A.S.T., Price, Z., Devaux, C., Hipperson, H., Smadja, C.M., Hutton, I., *et al.* (2013).  
423 A comparative analysis of the mechanisms underlying speciation on Lord Howe Island. *J.*  
424 *Evol. Biol.* 26: 733–745.

425 Poelstra, J.W., Vijay, N., Bossu, C.M., Lantz, H., Ryll, B., Müller, I., *et al.* (2014). The genomic  
426 landscape underlying phenotypic integrity in the face of gene flow in crows. *Science* (80-. ).  
427 344: 1410–1414.

428 R\_Development\_Core\_Team. (2019). R: a language and environment for statistical computing. R  
429 Foundation for Statistical Computing, Vienna, Austria.

430 Rafajlović, M., Emanuelsson, A., Johannesson, K., Butlin, R.K. & Mehlig, B. (2016). A universal  
431 mechanism generating clusters of differentiated loci during divergence-with-migration.  
432 *Evolution* (N. Y). 70: 1609–1621.

433 Ravinet, M., Faria, R., Butlin, R.K., Galindo, J., Bierne, N., Rafajlović, M., *et al.* (2017).  
434 Interpreting the genomic landscape of speciation: a road map for finding barriers to gene flow.  
435 *J. Evol. Biol.* 30: 1450–1477.

436 Renaut, S., Grassa, C.J., Yeaman, S., Moyers, B.T., Lai, Z., Kane, N.C., *et al.* (2013). Genomic  
437 islands of divergence are not affected by geography of speciation in sunflowers. *Nat. Commun.*  
438 4: 1827.

439 Samuk, K., Owens, G.L., Delmore, K.E., Miller, S.E., Rennison, D.J. & Schluter, D. (2017). Gene  
440 flow and selection interact to promote adaptive divergence in regions of low recombination.  
441 *Mol. Ecol.* 26: 4378–4390.

442 Savolainen, V., Anstett, M.-C., Lexer, C., Hutton, I., Clarkson, J.J., Norup, M. V, *et al.* (2006).  
443 Sympatric speciation in palms on an oceanic island. *Nature* 441: 210–213.

444 Simão, F.A., Waterhouse, R.M., Ioannidis, P., Kriventseva, E. V. & Zdobnov, E.M. (2015).  
445 BUSCO: Assessing genome assembly and annotation completeness with single-copy  
446 orthologs. *Bioinformatics* 31: 3210–3212.

447 Soria-Carrasco, V., Gompert, Z., Comeault, A.A., Farkas, T.E., Parchman, T.L., Johnston, J.S., *et*  
448 *al.* (2014). Stick Insect Genomes Reveal Natural Selection’s Role in Parallel Speciation.  
449 *Science* (80-. ). 344: 738–742.

450 Stanke, M., Schöffmann, O., Morgenstern, B. & Waack, S. (2006). Gene prediction in eukaryotes  
451 with a generalized hidden Markov model that uses hints from external sources. *BMC*  
452 *Bioinformatics* 7: 62.

453 Sundaresan, V. & Alandete-Saez, M. (2010). Pattern formation in miniature: the female  
454 gametophyte of flowering plants. *Development* 137: 179–189.

455 Tang, H., Zhang, X., Miao, C., Zhang, J., Ming, R., Schnable, J.C., *et al.* (2015). ALLMAPS:  
456 robust scaffold ordering based on multiple maps. *Genome Biol.* 1–15.

457 Turner, T.L. & Hahn, M.W. (2010). Genomic islands of speciation or genomic islands and  
458 speciation? *Mol. Ecol.* 19: 848–850.

459 Via, S. (2009). Natural selection in action during speciation. *Proc. Natl. Acad. Sci.* 106: 9939–9946.

460 Via, S. & West, J. (2008). The genetic mosaic suggests a new role for hitchhiking in ecological  
461 speciation. *Mol. Ecol.* 17: 4334–4345. Blackwell Publishing Ltd.

462 Weir, B.S. & Cockerham, C.C. (1984). Estimating F-statistics for the analysis of population  
463 structure. *Evolution (N. Y.)* 38: 1358–1370. Society for the Study of Evolution.

464 Woodroffe, C.D., Kennedy, D.M., Brooke, B.P. & Dickson, M.E. (2006). Geomorphological  
465 evolution of Lord Howe Island and carbonate production at the latitudinal limit to reef growth.  
466 *J. Coast. Res.* 22: 188–201. Coastal Education and Research Foundation.

467 Wu, C.I. (2001). The genic view of the process of speciation. *J. Evol. Biol.* 14: 851–865.

468

469

470

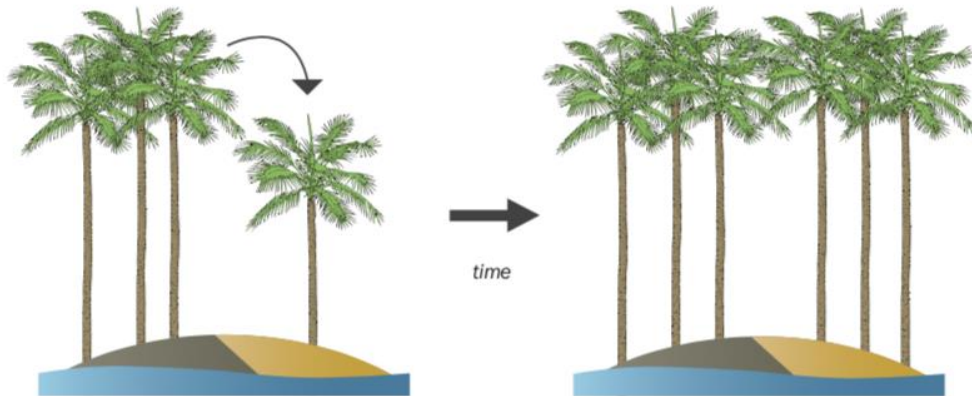
471

472

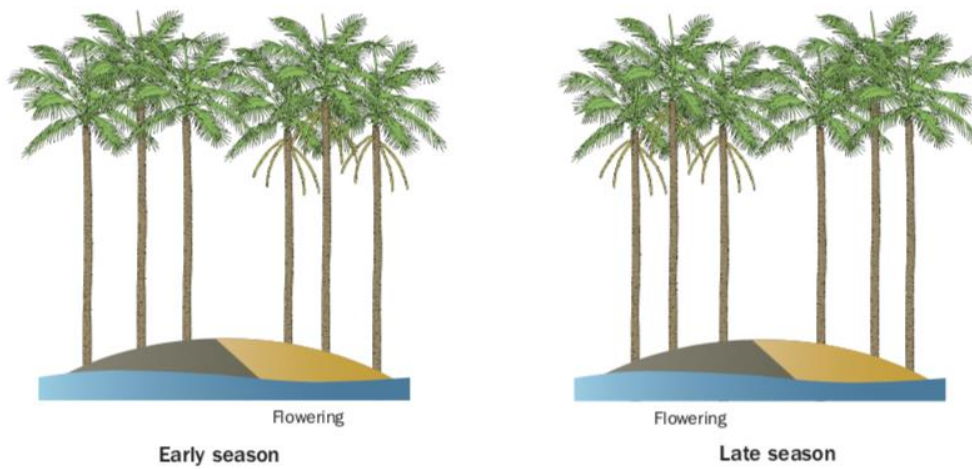
473



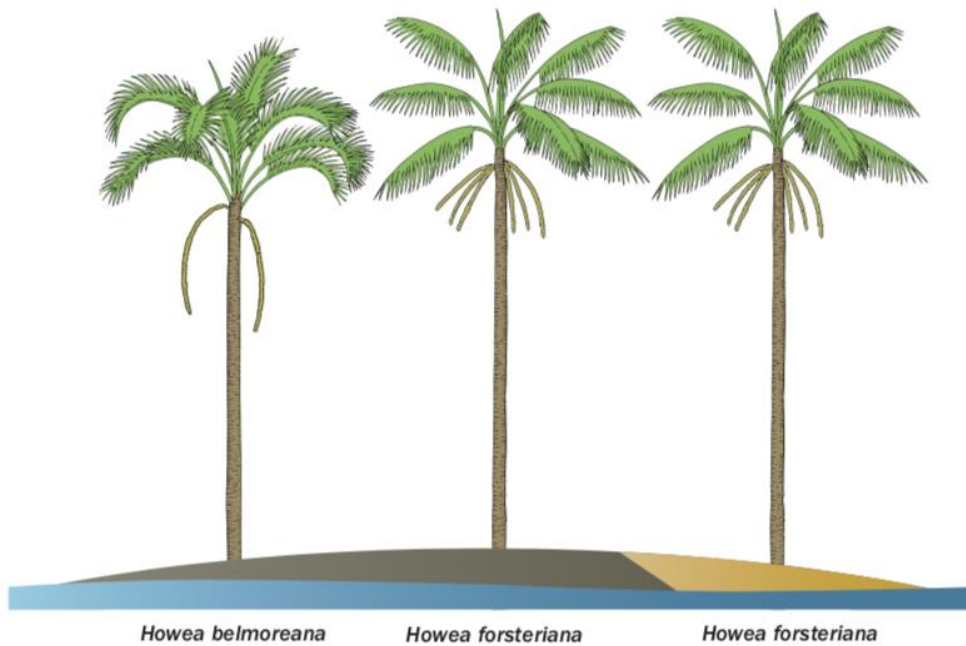
1. Ancestral *Howea* colonises calcarenite soils (disruptive selection)



2. Assortative mating via flowering time differences promotes species divergence (speciation)



3. Speciation is followed by further phenotypic, physiological and genetic divergence



475 **Fig. 1** Hypothesised speciation scenario for *Howea*. (1) Lord Howe Island is composed of two main  
476 soil types, volcanic (the initial soil type; dark brown) and calcareous soils (subsequent calcarenite  
477 deposits; light brown). An ancestral *Howea* colonised Pleistocene calcarenite deposits from  
478 volcanic soils, resulting in disruptive selection via adaptation to environmental stresses (e.g.,  
479 stemming from soil preferences) and triggering flowering time differences. (2) Assortative mating  
480 via displacement of flowering phenology promoted reproductive isolation. (3) Further divergence  
481 arose after speciation. Today, the curly palm, *H. belmoreana*, grows on volcanic soils, has erect  
482 leaflets, a single spike per inflorescence, and flowers late in the season. The kentia palm, *H.*  
483 *forsteriana*, has colonised both calcareous and volcanic soils, has pendulous leaflets, multiple  
484 spikes per inflorescence, and it flowers earlier in the season; it is also one of the world's most  
485 commonly traded houseplants.  
486

487  
488  
  
489  
490  
491  
492  
493  
494  
495  
496  
497  
498  
499  
500  
501  
502

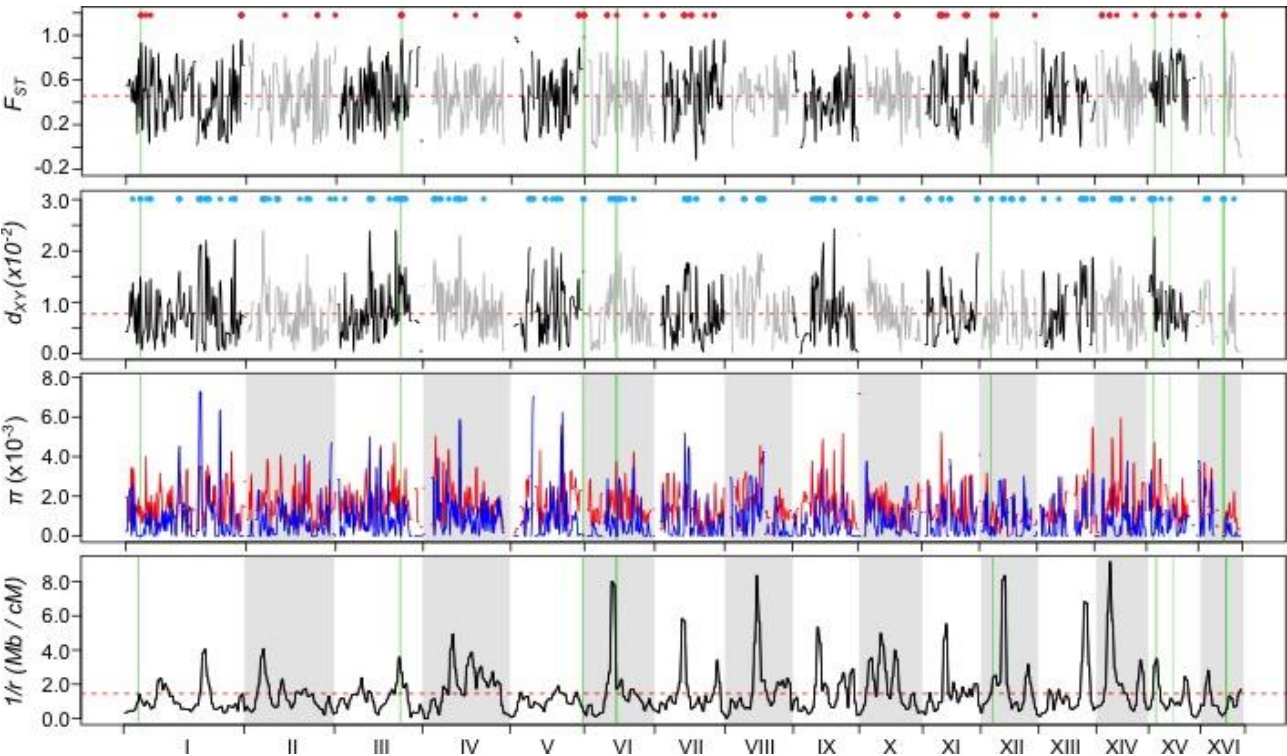


**Fig. 2** Genomic divergence between *H. belmoreana* and *H. forsteriana*. The x-axis denotes the genomic order of ddRAD markers on each chromosome. Chromosomes are ordered by length in cM. In the  $F_{ST}$  and  $d_{XY}$  plots (top two panels) kernel smoothed values of  $F_{ST}$  and  $d_{XY}$  on each chromosome are shown in alternately black and grey for adjacent chromosomes, coloured dots denote the positions of outlier positions (red =  $F_{ST}$  and blue =  $d_{XY}$ ), dashed red lines denote the genome average. Vertical green bars signify the positions of the 15 high- $F_{ST}+d_{XY}$  islands more likely involved in sympatric speciation, and red dots are the high- $F_{ST}$  only islands more likely to have occurred post-speciation (see text). Genetic diversity ( $\pi$ ) for *H. belmoreana* and *H. forsteriana* are shown by red and blue lines, respectively. The lower panel shows the recombination rate in 10cM windows. High- $F_{ST}$  and high- $F_{ST}+d_{XY}$  islands appear to be associated with regions of low recombination (i.e., low cM per Mb; high  $1/r$ ), but this association is not statistically significant. Note that genetic diversity is not lower in speciation islands despite low recombination.

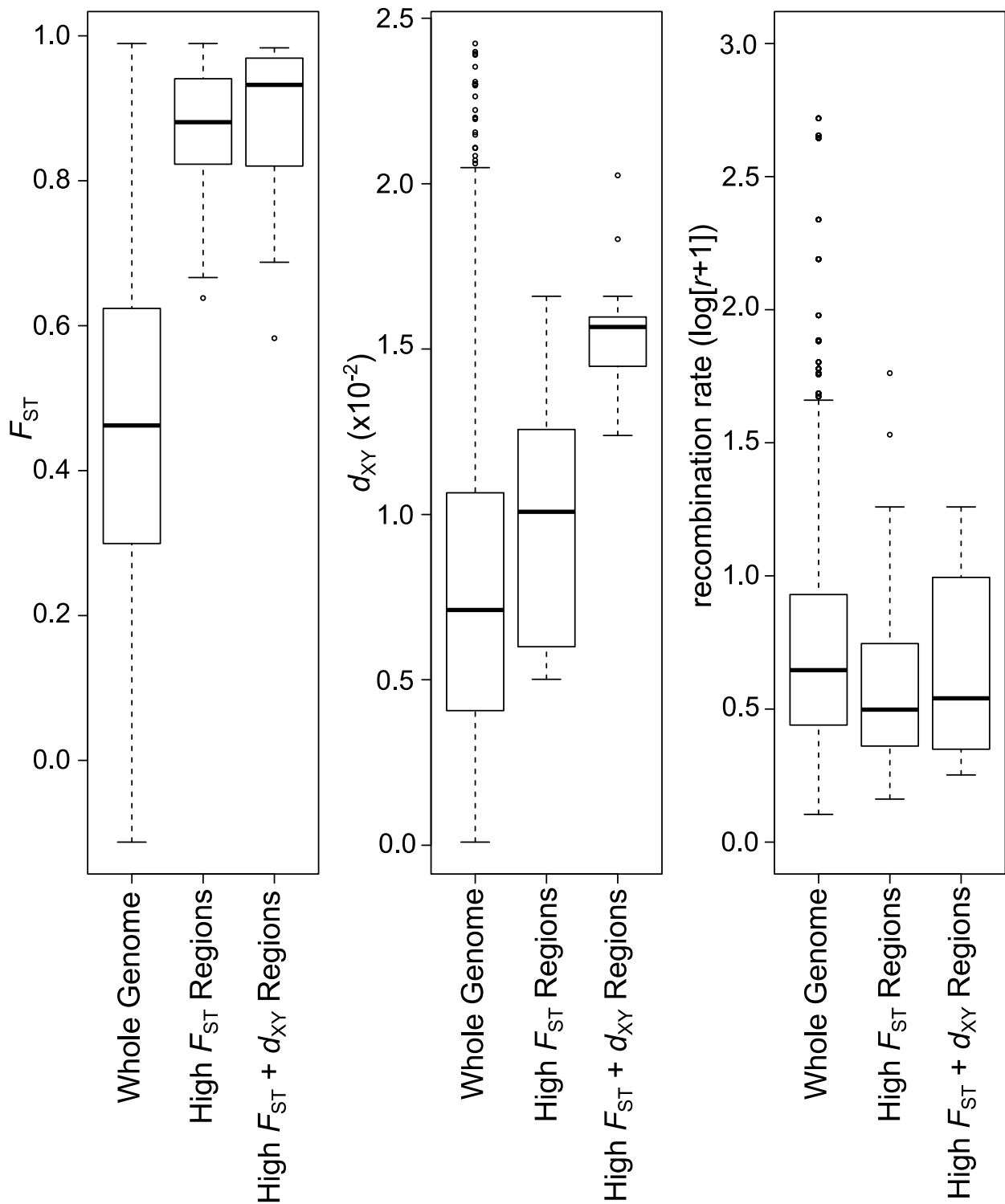


**Fig. 3** Comparison of divergence metrics. Boxplots depict the median (bold line), interquartile range (box), and 1.5 times the interquartile range (whiskers).

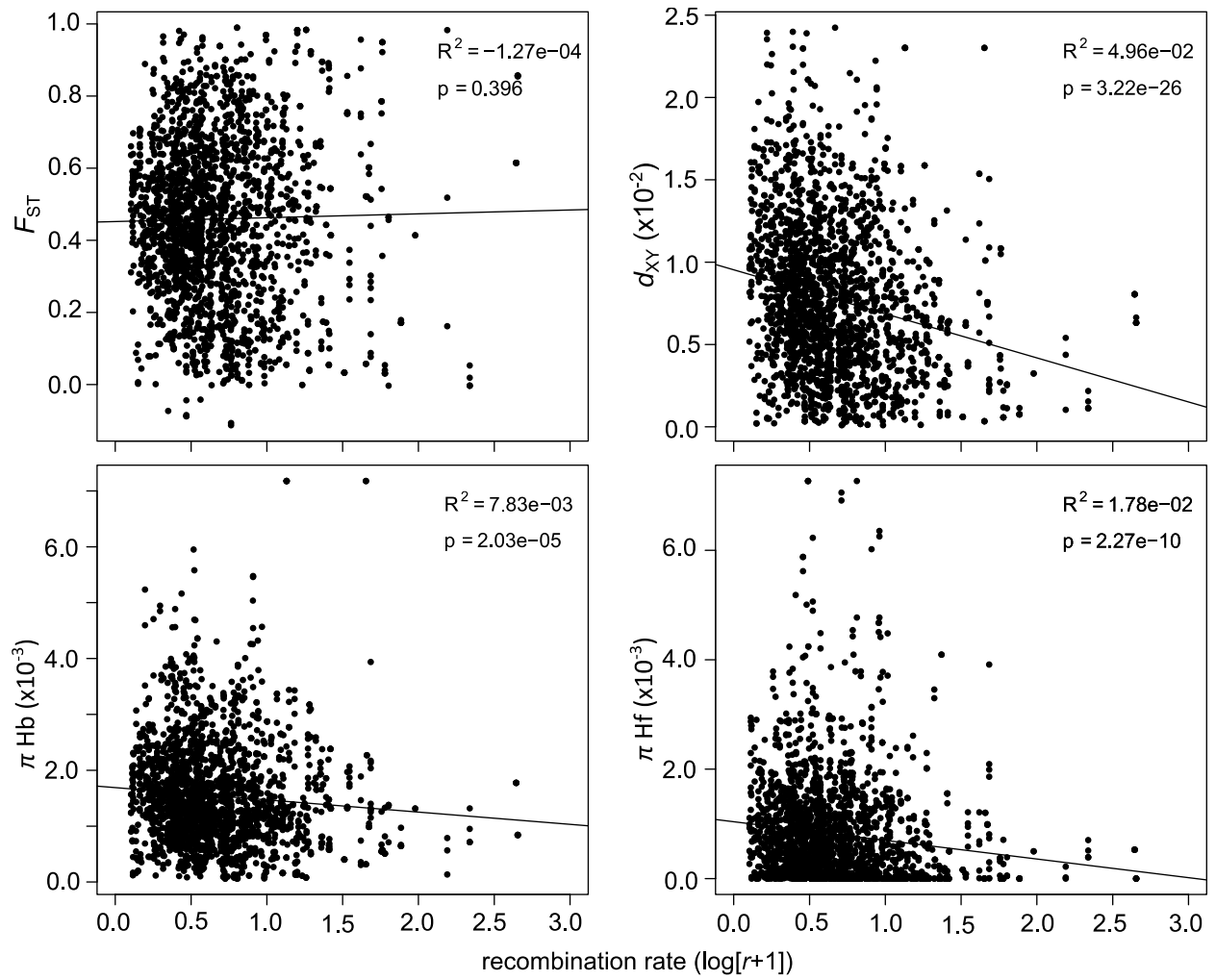


**Fig. 4** Genome wide relationships of recombination rate with population genetic metrics indicate no role for linked selection in shaping differentiation in *Howea*. Recombination rate was not correlated with  $F_{ST}$  but was negatively correlated with  $d_{XY}$  and  $\pi$  in both species.